Hindawi Publishing Corporation
Journal of Electrical and Computer Engineering
Volume 2015, Article ID 864508, 7 pages
http://dx.doi.org/10.1155/2015/864508

Research Article

Micro-Doppler Ambiguity Resolution Based on Short-Time Compressed Sensing

Jing-bo Zhuang, Zhen-miao Deng, Yi-shan Ye, Yi-xiong Zhang, and Yan-yong Chen

School of Information Science and Engineering, Xiamen University, Xiamen 361005, China

Correspondence should be addressed to Zhen-miao Deng; dzm_ddb@xmu.edu.cn

Received 4 May 2015; Revised 5 August 2015; Accepted 5 August 2015

Academic Editor: Igor Djurović

When using a long range radar (LRR) to track a target with micromotion, the micro-Doppler embodied in the radar echoes may suffer from ambiguity problem. In this paper, we propose a novel method based on compressed sensing (CS) to solve micro-Doppler ambiguity. According to the RIP requirement, a sparse probing pulse train with its transmitting time random is designed. After matched filtering, the slow-time echo signals of the micromotion target can be viewed as randomly sparse sampling of Doppler spectrum. Select several successive pulses to form a short-time window and the CS sensing matrix can be built according to the time stamps of these pulses. Then performing Orthogonal Matching Pursuit (OMP), the unambiguous micro-Doppler spectrum can be obtained. The proposed algorithm is verified using the echo signals generated according to the theoretical model and the signals with micro-Doppler signature produced using the commercial electromagnetic simulation software FEKO.

1. Introduction

Estimating and extracting micromotion information have attracted much attention in recent years [1–6]. Micromotion can be defined as the mechanical vibration, rotation, or other higher order motion components, excluding translational motion, of a target and will produce a frequency modulation on the returned signal that generates sidebands about the target's Doppler frequency. This is known as the micro-Doppler effect. This effect reflects the unique dynamic and structural characteristics of the target, which offers an approach for the recognition and identification of specific targets [7].

In Synthetic Aperture Radar (SAR)/Inverse Synthetic Aperture Radar (ISAR) imagery, micro-Doppler effect will introduce nonstationary phase modulation into returned signals, which will significantly decrease the readability of images [5, 8, 9]. In [8], an estimation method based on the discrete fractional Fourier transform is proposed to estimate the instantaneous vibration accelerations and frequencies. To separate the rigid body and the micro-Doppler parts, an L-statistics-based method for micro-Doppler effects removal is proposed in [9].

Most of the previous researches assume that the probing frequency to a micromotion target is large enough and thus there is no Doppler ambiguity and micro-Doppler ambiguity. However, a long range radar usually works in low PRF, which causes serious Doppler ambiguity and micro-Doppler ambiguity. In [10, 11], a CS-based Doppler ambiguity resolution method is proposed. However, this method cannot be applied to resolve micro-Doppler ambiguities. Therefore, it is necessary to study how to extract the unambiguous micro-Doppler time-frequency spectrum when the PRF is low. In [12], the CS is employed to remove undesirable cross terms in the Wigner-Ville distribution of the micro-Doppler radar signature. However, the micro-Doppler ambiguity problem is not discussed.

To solve micro-Doppler ambiguity problem, we propose a novel method based on CS in this paper. According to the RIP requirement of the sensing matrix, a sparse pulse train with random time stamps is designed based on the fixed-PRF pulses. The echo signals after matched filtering can be viewed as randomly sparse sampling of the micro-Doppler spectrum. To reconstruct the micro-Doppler signature from the sparse samples, we propose a short-time-compressed-sensing time-frequency analysis method. A short-time window slides along the slow-time domain echo signals and the reconstruction algorithm OMP is applied within this window to reconstruct the micro-Doppler spectrum. Two kinds of echo signals, one generated according to the theoretical model and one

produced by the commercial electromagnetic simulation software FEKO, are used to verify the proposed algorithm.

2. Theory

2.1. Radar Echo Signal Model. The transmitted chirp signal can be modeled as

$$s_{\text{tran}}\left(\hat{t}, t_m\right) = \text{rect}\left(\frac{\hat{t}}{T_p}\right)\exp\left(j2\pi\left(f_c t + \frac{1}{2}\gamma\hat{t}^2\right)\right), \quad (1)$$

where $\text{rect}(u) = \begin{cases}1, & |u|\le 0.5\\ 0, & |u|>0.5\end{cases}$; f_c and γ are the center frequency and the chirp rate, respectively; T_p and $\hat{t}$ are the pulse width and fast time, respectively; $t = \hat{t} + t_m$ is the full time, where t_m denotes the slow time. The received echo signal $s_{\text{rec}}(\hat{t}, t_m)$ can be defined as

$$\begin{aligned} s_{\text{rec}}&\left(\hat{t}, t_m\right)\\ &= A\text{rect}\left(\frac{\hat{t} - 2R_t/c}{T_p}\right)e^{j\pi\gamma\left(\hat{t}-2R_t/c\right)^2}e^{-j(4\pi f_c/c)R_t}, \end{aligned} \quad (2)$$

where A is the backscattered field amplitude for the point scatter, c is the speed of electromagnetic wave propagation, and R_t is the instantaneous distance between the radar and the target. Performing matched filtering to the received signal and transforming the results into range-frequency domain yield

$$r\left(f_r, t_m\right) = A'\text{rect}\left(\frac{f_r}{B}\right)\exp\left(-j\frac{4\pi}{c}\left(f_r + f_c\right)R_t\right), \quad (3)$$

where B is the signal bandwidth. Ignoring the acceleration, jerk of the target, R_t can be approximated by

$$R_t \approx R_0 + vt_m + r_{\text{micro}}\left(t_m\right), \quad (4)$$

where R_0 is the distance between the target and radar at time t_0, v is the radial velocity, and $r_{\text{micro}}(t_m)$ is the micromotion of the target. Substituting (4) into (3) yields the slow-time domain echo signal:

$$r\left(f_d, t_m\right) = A''\exp\left[-j2\pi f_d\left(t_m\right)t_m\right], \quad (5)$$

where $A'' = A'\exp(2(f_r + f_c)R_0/c)$ and $f_d(t_m)$ is the Doppler frequency and can be written as

$$\begin{aligned} f_d\left(t_m\right) &= \frac{1}{2\pi}\frac{d\varphi\left(t_m\right)}{dt_m} = \frac{2}{\lambda}\frac{dr\left(t_m\right)}{dt_m}\\ &= \frac{2}{\lambda}\left[v + \frac{dr_{\text{micro}}\left(t_m\right)}{dt}\right] = f_{b\_d} + f_{m\_d}\left(t_m\right) \end{aligned} \quad (6)$$

which consists of two parts, that is, the Doppler frequency f_{b_d} caused by translational motion and the micro-Doppler frequency $f_{m\_d}(t_m)$ caused by micromotion.

2.2. Requirements of the PRF. According to the Nyquist-Shannon sampling theorem, for a band-limited baseband signal the sampling rate must be greater than or equal to two times the highest frequency of the signal. For a pulsed radar, the Doppler frequency $f_d(t_m)$ of the target is sampled with the sampling rate as the PRF. When the micro-Doppler frequency exceeds half of the PRF, the micro-Doppler ambiguity phenomenon will occur. Thus, the PRF must be greater than or equal to the highest micro-Doppler frequency shift.

In a short-time interval, $f_d(t_m)$ can be seen as a constant. If there are K scatterers each with different micro-Doppler frequencies, the echo signal can be rewritten as

$$r\left(f_d, t_m\right) = \sum_{k=1}^{K} A''\exp\left\{-j2\pi f_{dk}t_m\right\}. \quad (7)$$

If the PRF is smaller than $\max_{k=1,\ldots,K}\{f_{dk}\}$, the spectrum aliases will occur in (7). According to the sub-Nyquist sampling theorem [13] or CS theory, the sparse signal can be sampled at a rate lower than the Nyquist. The slow-time domain radar echo signal can be viewed as the scalar sum of K sinusoidal signals, which is sparse in frequency domain [14]. Thus, the requirement for PRF can be loosened. Next we briefly review the compressing sensing theory.

2.3. Compressed Sensing. The theory of compressed sensing shows that when the signal is sparse or compressible, the signal can be reconstructed accurately or approximately by gathering very few projective values of the signal. Suppose x ($x \in R^N$) is a k-sparse (has k nonzero values) or compressive signal after orthogonal mapping projection and s is the sparse representation of x; then a measurement matrix $\mathbf{\Phi}$, which is irrelevant with the orthogonal map $\mathbf{\Psi}$, could be built to measure x linearly, resulting in only M ($M \ll N$) measured values y ($y \in R^M$):

$$y = \mathbf{\Phi}x. \quad (8)$$

The dimension of y is less than that of x, so the equation has infinity solutions. By solving the optimal problem above, signal x can be approximately reconstructed. x is sparse in $\mathbf{\Psi}$ domain; that is,

$$x = \mathbf{\Psi}s. \quad (9)$$

Substituting (9) into (8) yields

$$y = \mathbf{\Phi}x = \mathbf{\Phi}\mathbf{\Psi}s = \mathbf{\Theta}s, \quad (10)$$

where $\mathbf{\Theta} = \mathbf{\Phi}\mathbf{\Psi}$ is called sensing matrix with $M \times N$ dimension. As long as $\mathbf{\Theta}$ satisfies the Restricted Isometry Property (RIP), the sparse signal s could be recovered from the measured values y.

Signal reconstruction is the process of recovering x from the linear measured values y. The simplest method is to solve the ℓ_0 norm:

$$\begin{aligned} &\min_{x\in R^N} \quad \|\tilde{x}\|_0\\ &\text{s.t.} \quad \mathbf{\Phi}\tilde{x} = y. \end{aligned} \quad (11)$$

It is optimal in theory but impractical in numerical computation, belonging to a nondeterministic polynomial (NP) hard

problem. Donoho and Elad proved that ℓ_1 norm and ℓ_0 norm minimizations are equivalent if the solution is sufficiently sparse [15]. ℓ_1 norm

$$\begin{aligned} \min_{x \in R^N} \quad & \|\tilde{x}\|_1 \\ \text{s.t.} \quad & \boldsymbol{\Phi}\tilde{x} = y \end{aligned} \tag{12}$$

is an optimization problem and could be solved using linear programming.

According to the description of Section 2.2, we know that the radar echo signals can be viewed as the scalar sum of sinusoidal signals and are sparse in frequency domain; thus, the compressed sensing can be utilized. The linear measurement y is a $M \times 1$ column vector, which is randomly extracted from the measurements of (7) with the corresponding random sampling time t_m. Since $r(f_d, t_m)$ is sparse in frequency domain, the Fourier basis is chosen as the basis matrix $\boldsymbol{\Psi}$ with its element defined by

$$\psi_{i,k} = \frac{1}{\sqrt{N}} \exp\left(-j2\pi \frac{ik}{N}\right), \quad 0 \le i,\ k \le N. \tag{13}$$

Extracting M rows corresponding to the random transmitted time t_m from the identity matrix $\mathbf{I}_{N\times N}$ yields the measurement matrix $\boldsymbol{\Phi}$. Thus, the sensing matrix $\boldsymbol{\Theta}$ ($\boldsymbol{\Theta} = \boldsymbol{\Phi}\boldsymbol{\Psi}$) is obtained by randomly extracting M row from the sparse matrix $\boldsymbol{\Psi}$ and meets the RIP property.

Generally, the value of M is related to the relevancy $u(\boldsymbol{\Phi}_{N\times N}, \boldsymbol{\Psi})$ between the sparse matrix $\boldsymbol{\Psi}$ and the measurement matrix $\boldsymbol{\Phi}$ and satisfies

$$M \ge C \cdot u^2\left(\boldsymbol{\Phi}_{N\times N}, \boldsymbol{\Psi}\right) \cdot K \cdot \log N, \tag{14}$$

where C is a constant and $u(\boldsymbol{\Phi}_{N\times N}, \boldsymbol{\Psi})$ is defined as [16]

$$u\left(\boldsymbol{\Phi}_{N\times N}, \boldsymbol{\Psi}\right) = \sqrt{N} \cdot \max_{1\le k,j\le N} \left|\left(\varphi_k, \psi_j\right)\right|. \tag{15}$$

The classical recovery algorithms of compressed sensing are Basis Pursuit and Greedy Matching Pursuit. BP algorithm is the global optimization algorithm which has several advantages including superresolution and stability, but it is also accompanied with high computational complexity. Greedy Matching Pursuit algorithm, such as Orthogonal Matching Pursuit (OMP), is a local optimization algorithm and has the low computational complexity and high level of localization accuracy. The characteristics of OMP, such as easy implementation and fast speed, make it a better choice than BP algorithm [16].

3. Short-Time Compressed Sensing

Doppler frequency shifts generally have the time-varying characteristic and should be analyzed via the joint time-frequency analysis technique. However, when the PRF is lower than the Nyquist, the traditional time-frequency analysis methods are invalid. According to the above theoretical analysis results and the time-variant properties of micro-Doppler, we design a window-weighted compressed sensing method. According to the RIP of the CS sensing matrix, a sparse pulse train is randomly extracted from traditional fixed repetition frequency pulses. By adding a random perturbation item to the transmitting time of each selected pulse, we can obtain a new transmitting time sequence, which is equivalent to those extracted from a high PRF pulse transmitting time set. Then the corresponding measurement matrix can be obtained according to the transmitting time sequence. After matched filtering to the radar echoes, a short-time window slides along the slow-time domain echo signals and the CS method is applied within this window to reconstruct the micro-Doppler spectrum. Similar to the short-time Fourier transform (STFT), we call this method as short-time compressed sensing.

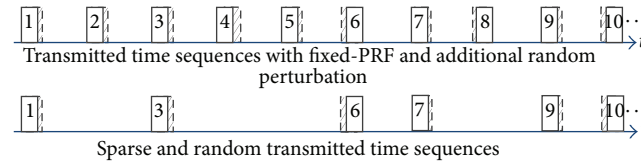

Figure 1: Illustration of radar dwell scheduling.

The PRF of a LRR is usually low. For a LRR working in fixed PRF mode, the slow-time domain echoes suffer from serious micro-Doppler ambiguity. By modifying the ith pulse transmitting time t_i to $t_i' = t_i + \Delta_i$, where Δ_i is a random perturbation, we can obtain a new transmitting time sequence. Since Δ_i is random, the equivalent PRF for t_i' is larger than that for t_i. The unambiguous micro-Doppler frequency range for t_i' will be larger than that for t_i since higher PRF means wider unambiguous micro-Doppler range.

When the value of M meets (14), the designed sensing matrix can satisfy the RIP property and the slow-time echo signals can be reconstructed based on the sparse measurements. Therefore, we can reduce the number of transmitted pulses by randomly selecting M pulses from the traditional fixed-PRF transmitted time sequences and adding a random perturbation to them. The building of sparse and random transmitted time sequences is demonstrated in Figure 1.

Since $f_d(t_m)$ is relevant to the slow time t_m, there is no applicable sensing matrix to reconstruct the micro-Doppler spectrum via compressed sensing directly. However, if we multiplied a short-time window to the slow-time echoes, $f_d(t_m)$ within this window can be seen as a constant and then the sensing matrix can be generated. Assuming the time precision is Δt, the corresponding equivalent PRF is $f_s' = 1/\Delta t$ and the Doppler unambiguous range for t_i' is represented as $f_s' = (1/\Delta t) f_s$. Thus, the unambiguous micro-Doppler frequency range expands to $(-f_s'/2, f_s'/2)$.

The signal within the window is written as

$$\tilde{r}\left(f_d, t_m\right) = w\left(t_n, t_m\right) \sum_{k=1}^{K} A'' \exp\left\{-j2\pi f_{dk}\left(t_n\right) t_n\right\}, \tag{16}$$

where the sliding short-time window is defined as $w(t_n, t_m) = \begin{cases} 1, & t_m \le t_n \le t_{m+L-1} \\ 0, & \text{else} \end{cases}$. In the window, the transmitted time sequence is $t_n \in \{t_m, t_{m+1}, \ldots, t_{m+L-1}\}$. The length of the window is

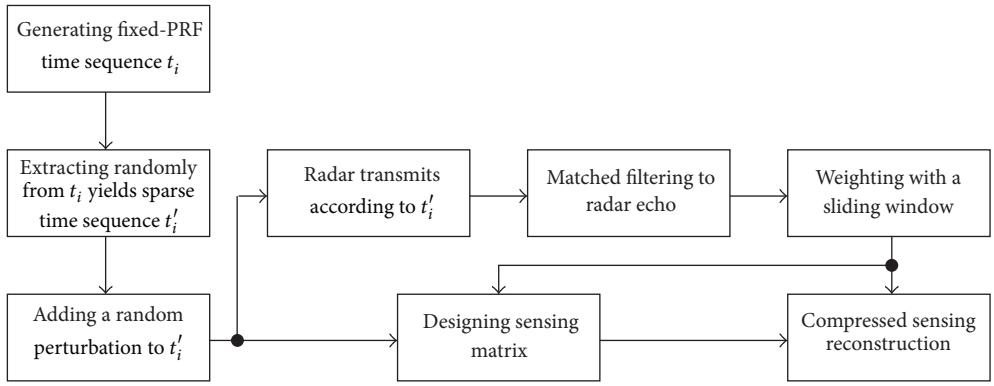

Figure 2: Flowchart of the proposed method.

L; that is, the length of the observed signal is $M = L$. In order to obtain more accurate Doppler estimate, an adaptive refinement algorithm of the sensing matrix proposed in [17] can be used to reconstruct the slow-time domain signal with higher precision. The column vector ψ_n of the basis matrix $\mathbf{\Psi} = [\psi_1, \psi_2, \ldots, \psi_N]$ is defined as $\psi_n(f) = \exp(j2\pi ft)$, and $\mathbf{\Psi}$ is an $N \times N$ matrix, where $N = 1/\Delta t$ and $\Delta f = (f_{\max} - f_{\min})/N$. According to t_n, extracting L rows from the basis matrix $\mathbf{\Psi}_{N\times N}$ yields the sensing matrix $\mathbf{\Theta}_{M\times N}$:

$$\mathbf{\Theta}_{M\times N} = \begin{bmatrix} e^{j2\pi f_0 t_0} & e^{j2\pi f_1 t_0} & \cdots & e^{j2\pi f_{N-1} t_0} \\ e^{j2\pi f_0 t_1} & e^{j2\pi f_1 t_1} & \cdots & e^{j2\pi f_{N-1} t_1} \\ \vdots & \vdots & \ddots & \vdots \\ e^{j2\pi f_0 t_{L-1}} & e^{j2\pi f_1 t_{L-1}} & \cdots & e^{j2\pi f_{N-1} t_{L-1}} \end{bmatrix}. \quad (17)$$

With the classical recovery algorithms, the unambiguous Doppler frequency $f_{dk}(t_m)$ can be reconstructed. Sliding the short-time window along the time axis and performing the CS operation, the unambiguous micro-Doppler time-frequency spectrum can be obtained.

To satisfy the RIP, the perturbation $\Delta_i = \varepsilon \cdot PRI$, where ε is a random variable uniformly distributed in $(0, 1)$; that is, $\varepsilon \sim U(0, 1)$. In practical application, there are two reasons causing that the term Δ_i could not be completely random: (1) the time sequence of radar is controlled by a reference clock. So the precision of Δ_i is limited to the precision of the clock; (2) theoretically, higher precision of Δ_i would yield larger unambiguous Doppler frequency range through refining the basis matrix. However, as pointed out in [14], the relationship between the DFT matrix refining factor, which is referred to the frequency redundancy factor, and the measurement number M should satisfy (20) in [14]. In other words, M would increase if the refining factor increases; therefore, the tradeoff between these two factors should be carefully considered. Furthermore, when the refining factor increases, the performance of recovery algorithm under noise environment will also degrade. Thus, we should carefully select proper Δt to ensure a good performance.

The process of the short-time compressed sensing on micro-Doppler spectrum reconstruction is summarized as follows:

(i) A new transmitting time sequence is generated by extracting randomly from the fixed-PRF transmitting time sequence. Then a perturbation is added to each element of the new transmitting time sequence. The radar transmits probing pulses according to the scheduled time sequence. Performing matched filtering to the echo pulses, the slow-time domain signals are obtained.

(ii) Slide a short-time window along the slow-time domain signals and construct the corresponding sensing matrix $\mathbf{\Psi}$ according to the time stamps of the window.

(iii) Performing the Orthogonal Matching Pursuit algorithm to the signals in the sliding window, the instantaneous micro-Doppler frequency is obtained.

The flowchart for the implementation of the algorithm is shown in Figure 2.

4. Simulation

In this section, simulations are performed to verify the proposed method. The proposed method can be applied to different kinds of micromotion. In the following, two micromotions, that is, spin and precession, are simulated.

Experiment 1 (one spin scatter case). The simulation parameters are shown in the list below. One scatter case is as follows.

Simulation Parameters

$f_c = 10$ GHz,
$B = 5$ MHz,
$f_r = 300$ Hz, $t = 2$ s,
$\omega = 2\pi$ rad/s,
$r_1 = 0.6$ m.

The corresponding slow-time echo signal for spin scatterers can be written as

$$r(f_d, t_m) = \sum_{k=1}^{1} A'' \exp\left\{-j2\pi \frac{2\omega_k r_k \cos(\omega_k t_m)}{\lambda} t_m\right\}. \quad (18)$$

The simulation results for spin motion are shown in Figure 3.

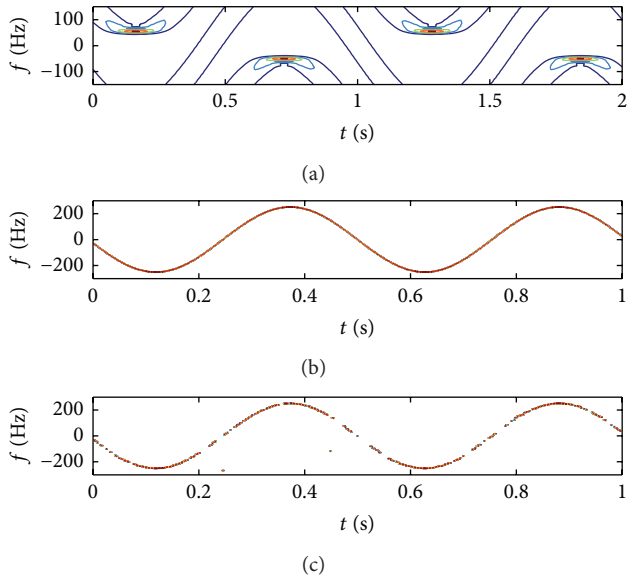

Figure 3: Micro-Doppler time-frequency spectrum: ambiguous time-frequency spectrum via STFT (a); unambiguous time-frequency spectrum of adding-perturbation fixed-PRF via CS (b); unambiguous time-frequency spectrum of adding-perturbation sparse-PRF via CS (c).

According to the simulated parameters, the maximum micro-Doppler frequency shift is ±250 Hz. Since the PRF is not large enough, the micro-Doppler spectrum obtained from the STFT is ambiguous. Add a random perturbation Δ_i to each time stamp of the transmitting time sequence $\{t_1, t_2, \ldots, t_n\}$, respectively. The accuracy of the perturbation is $\Delta t = 1.667e-4$ and the corresponding $\mathrm{PRF}' = 6000$. The length of the time window is $L = 10$; the number of measurements is $M = 10$; the length of the reconstructed signal is $N = 6000$; the sparse rate is $K = 2$; the sensing matrix $\boldsymbol{\Theta}$ is a 12×6000 matrix. The unambiguous micro-Doppler time-frequency spectrum can be recovered using the CS reconstruction algorithm, which is shown in (b) of Figure 3. Randomly selecting a portion of elements from $\{t_1, t_2, \ldots, t_n\}$ and adding a random perturbation Δ_i to each of the selected elements, we can generate sparse probing pulses. (c) of Figure 3 shows the unambiguous micro-Doppler spectrum reconstructed from these sparse pulses with good performance. The sparse rate, that is, the number of sparse probing pulses divided by the number of the original fixed-PRF pulses, is 0.6.

In order to investigate the effect of the number of measurements M on the reconstruction quality for a fixed sparse rate, we select different M values and compare the reconstruction results, which are shown in Figure 4. We can see that larger M corresponds to better reconstruction performance.

Experiment 2 (two spin scatterers' case). Two spin scatterers are simulated and the simulation parameters are shown in the list below. To demonstrate the ambiguity resolving ability of our method, we change the rotating radius $r_1 = 0.6$ m of Experiment 1 to $r_1 = 1.8$ m. With these simulation parameters, the micro-Doppler of this scatterer will be ambiguous

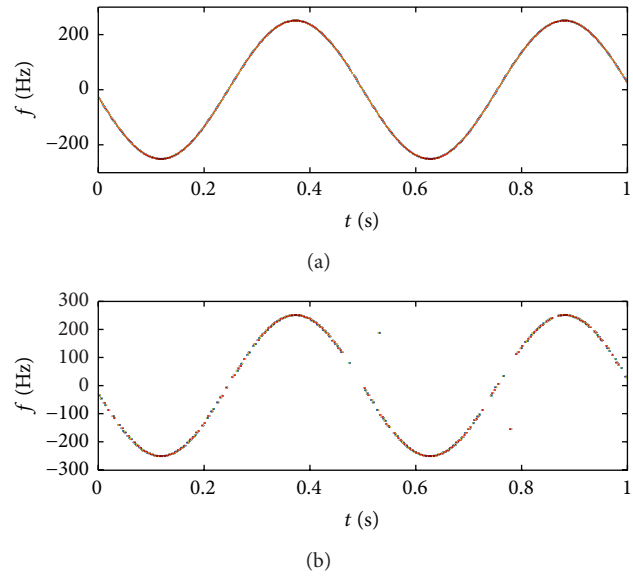

Figure 4: CS reconstruction quality with different measurement number. (a) $M = 10$; (b) $M = 6$.

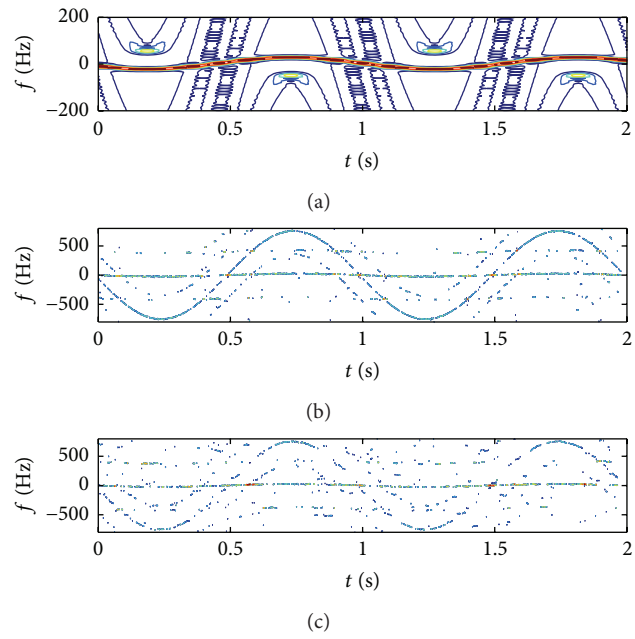

Figure 5: Micro-Doppler time-frequency spectrum: ambiguous time-frequency spectrum via STFT (a); unambiguous time-frequency spectrum of adding-perturbation fixed-PRF via CS (b); unambiguous time-frequency spectrum of adding-perturbation sparse-PRF via CS (c).

twice, which can be seen from (a) of Figure 5. Performing the short-time compressed sensing, the unambiguous micro-Doppler can be recovered successfully. The sparse rate of (c) of Figure 5 is 0.75.

Simulation Parameters

$$f_c = 10\,\mathrm{GHz},$$

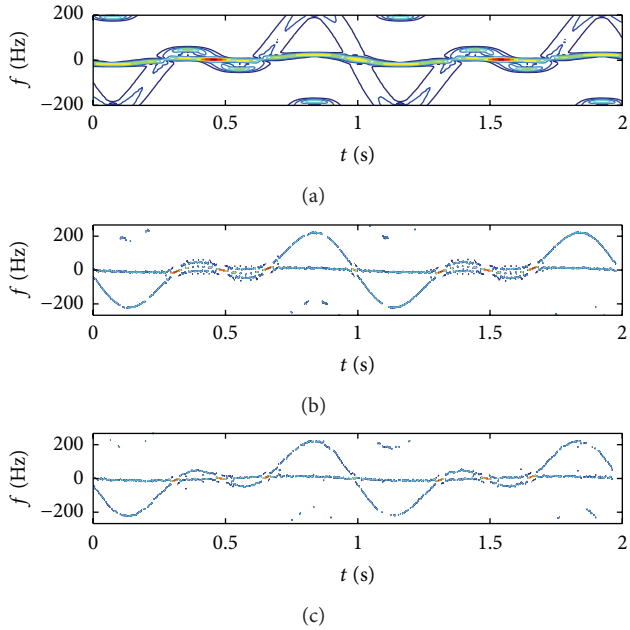

Figure 6: Micro-Doppler time-frequency spectrum: ambiguous time-frequency spectrum via STFT (a); unambiguous time-frequency spectrum of adding-perturbation fixed-PRF via CS (b); unambiguous time-frequency spectrum of adding-perturbation sparse-PRF via CS (c).

$$B = 5\,\text{MHz},$$
$$f_r = 400\,\text{Hz}, t = 2\,\text{s},$$
$$\omega = 2\pi\,\text{rad/s},$$
$$r_1 = 1.8\,\text{m}, r_2 = 0.06\,\text{m}.$$

Experiment 3 (two precession scatterers' case). Two precession scatterers are simulated and the simulation parameters are shown in the list below (19). The simulation results for precession motion can be shown in Figure 6. The corresponding slow-time echo signal for precession scatterers can be written as

$$r(f_d, t_m) = \sum_{k=1}^{2} A'' \cdot \exp\left\{-j2\pi\left[\frac{2\omega_1 r_k \cos(\omega_1 t_m)}{\lambda} + \frac{2\omega_2 R_k \cos(\omega_2 t)}{\lambda}\right] \cdot t_m\right\}. \quad (19)$$

Simulation Parameters

$$f_c = 10\,\text{GHz},$$
$$B = 5\,\text{MHz},$$
$$f_r = 400\,\text{Hz}, t = 2\,\text{s},$$
$$\omega_1 = 2\pi\,\text{rad/s}, \omega_2 = 4\pi\,\text{rad/s},$$
$$r_1 = 0.3\,\text{m}, R_1 = 0.15\,\text{m},$$
$$r_2 = 0.03, R_2 = 0.015.$$

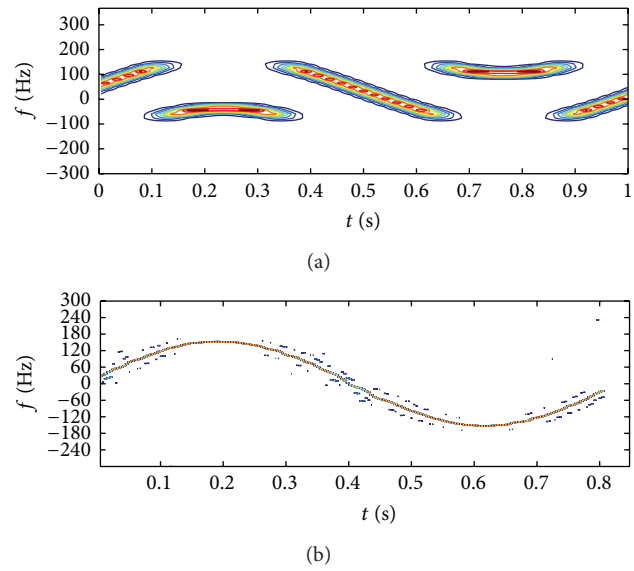

Figure 7: Micro-Doppler time-frequency spectrum: ambiguous time-frequency spectrum via STFT (a); unambiguous time-frequency spectrum of adding-perturbation sparse-PRF via CS (b).

The simulation results for the precession case are similar to those for the spin case. The sparse rate of (c) of Figure 6 is 0.5. The simulation results in Figures 3–6 show that the proposed method can expand the unambiguous micro-Doppler frequency range.

Experiment 4. In this experiment, we use the electromagnetic simulation software FEKO to generate sparse-sampled slow-time echo signals and reconstruct the unambiguous micro-Doppler spectrum via CS. A scatterer is rotating with a radius of 30 cm. The rate of angular motion is 2π rad/s. The carrier frequency is 10 GHz. The bandwidth is 500 MHz. The azimuth and pitch angle are 0° and 90°, respectively. The dynamic position of the scatterer at each sparse probing time stamp is calculated with MATLAB and then the corresponding slow-time echo is resolved with FEKO. The PRF is 200 Hz.

According to the configuration, the maximum micro-Doppler frequency is $f_{\max} = 40\pi$. Since the PRF $f_r < 2f_{\max}$, the micro-Doppler is ambiguous. The ambiguous micro-Doppler spectrum with fixed-PRF probing pulses is shown in (a) of Figure 7 and the unambiguous micro-Doppler spectrum with sparse-PRF probing pulses is shown in (b) of Figure 7. It can be seen that our proposed method is also suitable for the simulated echoes with FEKO.

5. Conclusion

The proposed short-time compressed sensing method can solve the micro-Doppler ambiguity problem. The sensing matrix built based on the sparse probing time stamps can meet the requirement of RIP property. Performing the OMP algorithm to the signals within the sliding short-time window, the ambiguous micro-Doppler spectrum can be reconstructed. The proposed method can work in low

PRF circumstances and requires transmitting fewer probing pulses while at the same time it can achieve larger unambiguous micro-Doppler range.

Conflict of Interests

The authors declare that there is no conflict of interests regarding the publication of this paper.

Acknowledgments

The research was supported by the National High-Tech R&D Program of China, the Open-End Fund National Laboratory of Automatic Target Recognition (ATR), the Open-End Fund of BITTT Key Laboratory of Space Object Measurement, and the National Natural Science Foundation of China (Grant no. 62101196).

References

[1] T. Thayaparan, L. J. Stanković, M. Daković, and V. Popović, "Micro-Doppler parameter estimation from a fraction of the period," *IET Signal Processing*, vol. 4, no. 3, pp. 201–212, 2010.

[2] K. Li, Y. Liu, K. Huo, W. Jiang, X. Li, and Z. Zhuang, "Estimation of micro-motion parameters based on cyclostationary analysis," *IET Signal Processing*, vol. 4, no. 3, pp. 218–223, 2010.

[3] T. Thayaparan, K. Suresh, S. Qian, K. Venkataramaniah, S. SivaSankaraSai, and K. S. Sridharan, "Micro-doppler analysis of a rotating target in synthetic aperture radar," *IET Signal Processing*, vol. 4, no. 3, Article ID ISPECX000004000003000245000001, pp. 245–255, 2010.

[4] T. Thayaparan, L. Stanković, and I. Djurović, "Micro-Doppler-based target detection and feature extraction in indoor and outdoor environments," *Journal of the Franklin Institute*, vol. 345, no. 6, pp. 700–722, 2008.

[5] Q. Wang, M. Pepin, A. Wright et al., "Reduction of vibration-induced artifacts in synthetic aperture radar imagery," *IEEE Transactions on Geoscience and Remote Sensing*, vol. 52, no. 6, pp. 3063–3073, 2014.

[6] P. Suresh, T. Thayaparan, T. Obulesu, and K. Venkataramaniah, "Extracting micro-doppler radar signatures from rotating targets using fourier-bessel transform and time-frequency analysis," *IEEE Transactions on Geoscience and Remote Sensing*, vol. 52, no. 6, pp. 3204–3210, 2014.

[7] L. Liu, D. McLernon, M. Ghogho, W. Hu, and J. Huang, "Ballistic missile detection via micro-Doppler frequency estimation from radar return," *Digital Signal Processing*, vol. 22, no. 1, pp. 87–95, 2012.

[8] S. B. Colegrove, S. J. Davey, and B. Cheung, "Separation of target rigid body and micro-Doppler effects in ISAR imaging," *IEEE Transactions on Aerospace and Electronic Systems*, vol. 42, no. 4, pp. 1496–1506, 2006.

[9] L. Stanković, T. Thayaparan, M. Daković, and V. Popović-Bugarin, "Micro-doppler removal in the radar imaging analysis," *IEEE Transactions on Aerospace and Electronic Systems*, vol. 49, no. 2, pp. 1234–1250, 2013.

[10] Y. H. Quan, L. Zhang, M. D. Xing, and Z. Bao, "Velocity ambiguity resolving for moving target indication by compressed sensing," *Electronics Letters*, vol. 47, no. 22, pp. 1249–1251, 2011.

[11] Y.-X. Zhang, J.-P. Sun, B.-C. Zhang, and W. Hong, "Doppler ambiguity resolution based on compressive sensing theory," *Journal of Electronics & Information Technology*, vol. 33, no. 9, pp. 2103–2107, 2011.

[12] N. Whitelonis and H. Ling, "Radar signature analysis using a joint time-frequency distribution based on compressed sensing," *IEEE Transactions on Antennas and Propagation*, vol. 62, no. 2, pp. 755–763, 2014.

[13] M. Mishali and Y. C. Eldar, "Sub-nyquist sampling," *IEEE Signal Processing Magazine*, vol. 28, no. 6, pp. 98–124, 2011.

[14] M. F. Duarte and R. G. Baraniuk, "Spectral compressive sensing," *Applied and Computational Harmonic Analysis*, vol. 35, no. 1, pp. 111–129, 2013.

[15] D. L. Donoho and M. Elad, "Optimally sparse representation in general (nonorthogonal) dictionaries via ℓ_1 minimization," *Proceedings of the National Academy of Sciences of the United States of America*, vol. 100, no. 5, pp. 2197–2202, 2003.

[16] J.-H. Wang, Z.-T. Huang, Y.-Y. Zhou et al., "Generalized incoherence principle in compressed sensing," *Signal Processing*, vol. 28, no. 5, pp. 675–679, 2012.

[17] L. Hu, Z. Shi, J. Zhou, and Q. Fu, "Compressed sensing of complex sinusoids: an approach based on dictionary refinement," *IEEE Transactions on Signal Processing*, vol. 60, no. 7, pp. 3809–3822, 2012.